2021

Osmocean

Katie Brodersen

Alec Lanter

Maulee Sheth

Nathaniel Kiefer

Emily Bywater

See next page for additional authors

Recommended Citation

Brodersen, Katie; Lanter, Alec; Sheth, Maulee; Kiefer, Nathaniel; Bywater, Emily; Furia, Kumansh; Cafferty, Brittany; Schennum, Hayden; Xie, Yi; Werner, Abigail; Ramchandani, Deepika; Cordoba, Sandra; Rao, Akshay; Chen, Jun; Das, Abhimanyu; and Warsinger, David M., "Osmocean" (2021). *School of Mechanical Engineering Working Papers.* Paper 4.
https://docs.lib.purdue.edu/mewp/4

Authors

Katie Brodersen, Alec Lanter, Maulee Sheth, Nathaniel Kiefer, Emily Bywater, Kumansh Furia, Brittany Cafferty, Hayden Schennum, Yi Xie, Abigail Werner, Deepika Ramchandani, Sandra Cordoba, Akshay Rao, Jun Chen, Abhimanyu Das, and David M. Warsinger

Marine Energy Collegiate Competition 2021

Written Report

Purdue University

Submitted to:

National Renewable Energy Laboratory

U.S. Department of Energy

Submitted by:

Purdue MECC

kbroders@purdue.edu

April 16, 2021

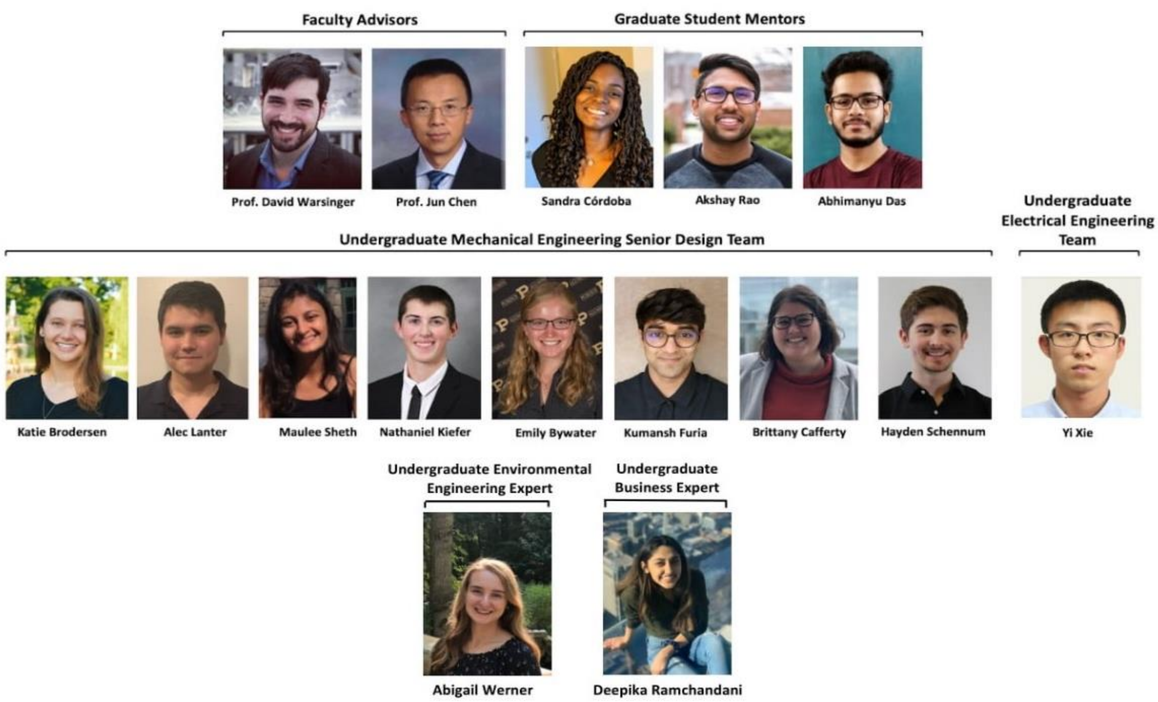

Nomenclature:

AWP: Annual Water Production
BRO: Batch Reverse Osmosis
BVI: British Virgin Islands
CapEx: Capital Expenditures
CDC: Center for Disease Control and Prevention
CRO: Continuous Reverse Osmosis
FOS: Factor of Safety
GWP: Global Warming Potential
LCA: Life Cycle Assessment
LCI: Life Cycle Inventory
LCOW: Levelized Cost of Water
LMH: Liters per square meter per hour; measure of flux
MECC: Marine Energy Collegiate Competition
NRD: Natural Resource Depletion
NREL: National Renewable Energy Laboratory
OpEx: Operating Expenditures
OSWEC: Oscillating Surge WEC
P&ID: Piping and instrumentation diagram
PID: Proportional Integral Derivative
PRO: Pressure Retarded Osmosis
PTO: Power Take-Off
RES: Renewable Energy Source
RO: Reverse Osmosis
RTF: Run-to-Failure
SEC: Specific Energy Consumption
SS: Stainless Steel
SWRO: Sea Water Reverse Osmosis
WEC: Wave Energy Converter

Executive Summary

The United Nations predicts that 6 billion people will face water scarcity by 2050. Of these, 40% of people live within 100 km from a coast [1]. The Purdue MECC team designed the first wave-powered batch desalination process, which allows for high-efficiency water production without the need for grid infrastructure. This report highlights the design process executed and business considerations made by the team in developing the *Osmocean* system.

Osmocean is the integration of wave energy and batch reverse osmosis (BRO)[17,18], which includes a BRO system, coupling (PTO) system, and WEC (not designed by the Purdue MECC team). BRO is the most efficient RO configuration realizable [39], and the *Osmocean* system is the first to scale up this technology. The system harnesses wave energy mechanically, without a transmission to electrical power, to couple with BRO.

Interviewing a wide range of potential clients provided insight on how to design a system to serve the most customers possible. Through rigorous engineering optimization and high-fidelity dynamic simulation, the team has proven that the system can reliably adapt to various sea states while maintaining a low specific energy consumption. The system sustains itself on wave energy alone, avoiding the environmental harm and efficiency losses associated with electric grids and non-renewable energy. *Osmocean* poses minimal environmental threat as its constituent materials and working fluid (seawater) do not pollute local waters.

A three-stage strategy for commercialization was developed that involves partnering with prominent RO and WEC developers and using existing infrastructure for prototyping. This model supports revenue generation through small-scale deployment while identifying critical size-capacities required for cost-competitive full-scale deployment. Thorough technoeconomic analysis shows that *Osmocean* has potential to be the most cost-competitive wave-desalination system on the market and could compete with other renewable energy sources.

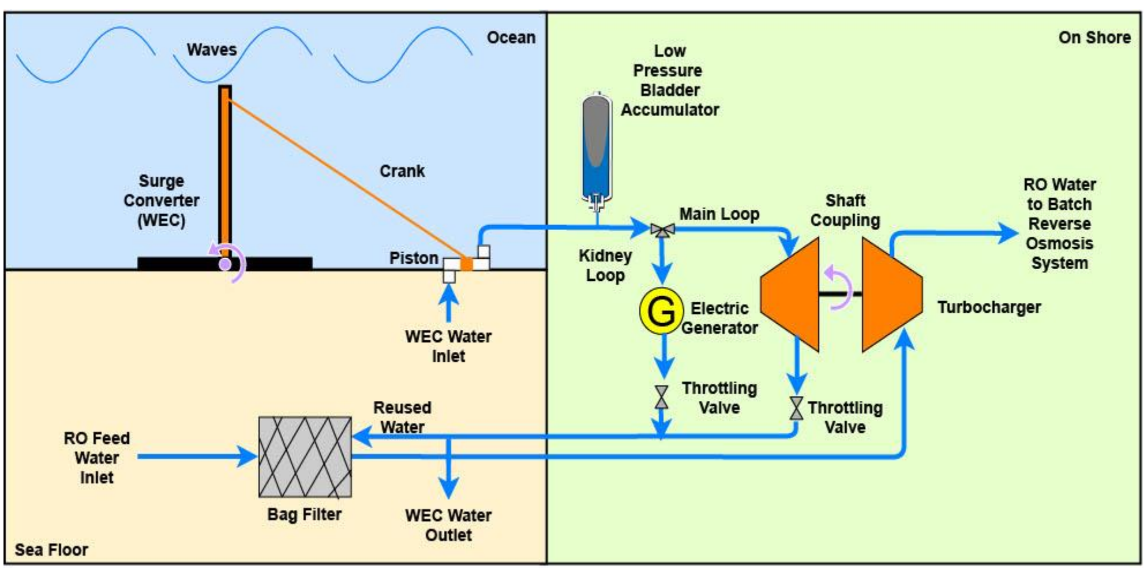

Figure 1: Graphical Abstract of the *Osmocean* system prior to BRO. Pressurized water is divided into a main loop that powers a turbocharger and a kidney loop that diverts flow from the main line. An electric generator powers the control system of *Osmocean* and the circulation pump in BRO. RO feed water is pressurized by the turbocharger.

BUSINESS PLAN

B.1 Concept Overview

Osmocean is a low-cost, self-sustaining, and energy-efficient system that is fully powered by wave energy. The *Osmocean* system directly links water pressurized by a wave energy converter (WEC) to an onshore batch reverse osmosis (BRO) system mechanically, via a power take-off (PTO) coupling. BRO is a novel configuration of reverse osmosis (RO) that achieves efficiencies higher than any other version of RO. The team has partnered with the Warsinger Water Lab, the leading BRO research group, which investigates a multitude of water science technologies. BRO facilitates energy savings as compared to RO, hence the *Osmocean* PTO coupling has the potential to be the most efficient PTO on the market. *Osmocean* is mechanically simple, consisting primarily of an accumulator, a turbocharger mechanism, two throttle valves, and an electrical generator to power all valves and sensors. The direct coupling of waves-to-BRO ensures that maximum energy is harvested and that nothing is left reliant on non-renewable fuel sources. In a future where water insecurity and climate change pose an ever-growing threat, *Osmocean* is a viable alternative to today's desalination systems.

The value proposition of *Osmocean* is the integration of wave energy and BRO. The *Osmocean* system is a proof-of-concept that wave energy can be harnessed mechanically, without a transmission to electrical power, to couple with BRO. This system is the first product to feature scaled up BRO technology. Furthermore, the use of a turbocharger, a common part in gas power industries, is a novel energy recovery plan for hydraulic systems. The design employs an innovative control strategy using throttling valves to control flow and pressure in the system. Hence, *Osmocean* builds upon the existing technologies of WEC and BRO.

B.2 Market Deployment Feasibility

B.2.1 Market Opportunity

The desalination market has grown in capacity by 20% between 2016 and 2020 [2], and it will continue to grow as population increases and freshwater sources are depleted. Of the many and varied renewable energy sources (RES), marine energy stands out for its ubiquity and ease of access by large swathes of the world population. When selecting a system, the mechanical and cost efficiency of different wave-powered desalination systems can be used to evaluate their performances. Resolute Marine estimates a levelized cost of water (LCOW) of 1.30/m^3 for their Wave2O™ system [3] and Wavepiston's estimated LCOW is \$1.80/m^3 [4]. In 2017, NREL researchers conducted a baseline study of WEC desalination farms and arrived at \$1.82/m^3 for a system that generates 3100 m^3/day of water [8]. The LCOW of *Osmocean* was estimated as \$1.94/m^3 for a scale of 2600 m^3/day. While the modeled LCOW is higher than currently published results, this is due to desirable mechanical simplicity (T.9: Optimization Methods).

B.2.2 Relevant Stakeholders and End Users

Osmocean's business model aims to address the desalination sector of the blue economy in three market stages (Figure B.2.2.0). The business plan involves initially marketing to the target market, then expending to the expansion market, and finally targeting the total addressable market. Customer discovery and interviews are discussed in section B.3.

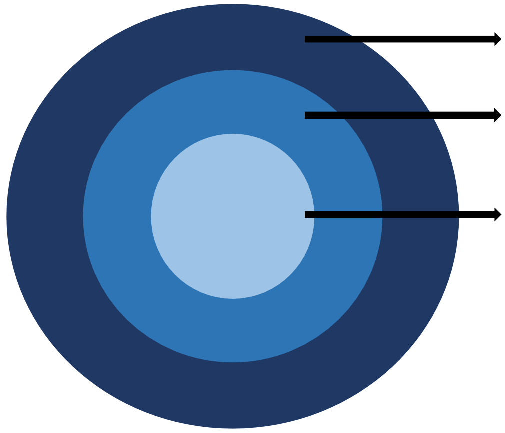

Figure B.2.2.0: Diagram illustrating the target, expansion, and total addressable markets. The target market circle will expand as time progresses.

B.2.2.1 Target Market

The target market refers to existing wave-powered RO companies that use standard CRO processes, such as Resolute Marine, and WEC developers that can couple WEC systems with *Osmocean*. The initial marketing phase involves proposing the idea of retrofitting batch-reverse osmosis processes to existing commercial processes. This allows for a low-capital approach to demonstrate a proof-of-concept with already-profitable infrastructure, noting that WECs are expensive to develop [8]. This target market will allow *Osmocean* to generate revenue while the system is perfected.

B.2.2.2 Expansion Market

The expansion market (remote island residents, governments, hotels, and non-profits) allows deployment of *Osmocean* at larger scales. Once initial revenue is built from the target market phase, the aim will be to implement a full-scale system, first focusing on small remote island communities such as Hawaii, Caribbean, the Philippines, and Greece (B.3: Customer Discovery). This strategy is in place because isolated communities tend to rely on expensive imported diesel fuel to power water treatment and are thus in the most need of a more fiscally and environmentally sustainable alternative. The *Osmocean* development team will act as a design firm working with local municipalities and contractors at local construction firms, and the plan is to deploy a system in 1 to 5 years. The entire life cycle of a desalination plant build can last for up to 25 years, as shown by customer discovery interviews with Webcor construction in California (B.3).

B.2.2.3 Total Addressable Market

The total addressable market includes the larger goal of bringing *Osmocean* to all coastal communities who desire this system (i.e. when the expansion market is saturated). Cost-effective development at this scale relies on the maturation of wave energy conversion technology, such that costs are eventually reduced to the point of being competitive with other traditional renewables. Purdue MECC's long-term business goal is to serve coastal regions across the globe.

B.2.3 Cost Competitiveness with Alternative Energy Sources

From a sustainability standpoint, several renewable energy sources (RES) are prospects for powering a sea water reverse osmosis (SWRO) desalination system: wind, solar, and wave energy [7]. Of the three, wave energy is the least developed. It follows that components of wave energy systems may not be as optimized relative to components of wind and solar energy from an efficiency and cost standpoint. That said, sensitivity analyses suggest that when countries allocate more funding to the advancement of RES, the levelized cost of water produced by methods of RES decreases [7]. According to Global Water Intelligence, US CapEx in desalination technology doubled within five years, from $129 million in 2015 to $344 million in 2020 [2]. With such a massive increase in such a short period of time, the desalination market is likely to increase in capacity as competition spurs innovation in all facets of desalination – wave energy included. As it currently stands, the LCOW for wind energy SWRO is about $1.80/m^3 for large-scale systems [6], and the LCOW for solar energy SWRO is estimated to be $0.35/m^3 [5]. The LCOW of a wave-powered desalination system features the same WEC device as *Osmocean* was calculated to be $1.82/m^3 (confirmed by the authors) [8]. Therefore, the team expects the LCOW of a refined *Osmocean* to be close to this figure, with the goal of being lower.

B.2.4 Development and Operations

The development of *Osmocean* included an analysis of how supply chain would be executed via Figure B.2.4.0. This supply-chain process will be different during the stages of initial deployment in which only PTO raw materials or BRO raw materials may be retrofitted to existing systems.

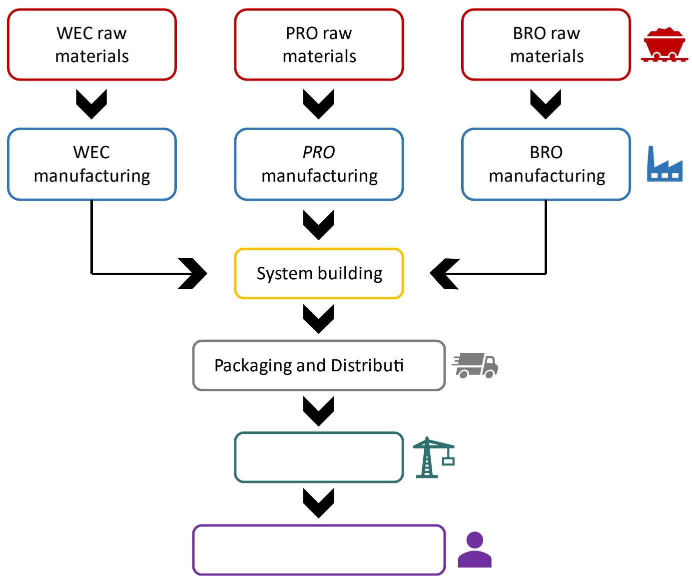

Figure B.2.4.0: Supply chain diagram illustrating the development of the *Osmocean* from the perspective of all the components from raw materials (red) through manufacturing (blue) through system assembly (yellow) through transportation (gray) through deployment (teal) through customer use (purple).

B.2.4.1 Research and Development (R&D)

The 2021 MECC provided the financial support for the *Osmocean* concept to be established. A project in its nascency, *Osmocean* will require additional funding and manpower to grow. The current Purdue MECC team has been recruiting students to carry the project forward and compete in future MECC cycles, which will be elaborated upon during the Communications & Outreach portion of the public pitch at ICOE. The inaugural team has proven that a WEC can effectively be coupled with BRO, but future work is essential to identify the most efficient system scale for different locations. With such an innovative coupling design and control strategy between wave power and BRO, the team plans to form partnerships with researchers and companies with established expertise in wave energy and deployment of wave-powered desalination in coastal markets.

B.2.4.2 Partnerships

Dr. Matt Folley, a senior hydrodynamic engineer, has provided invaluable modeling advice. Linda Rauch, a process engineer, helped the team access data from the DesalData cost estimator. For further expansion of *Osmocean*, the team will leverage existing connections with Resolute Marine, a leading company in wave-powered RO. Discussions of partnerships on future work have taken place but require a longer time frame.

The team established a partnership with the Swagelok Company to provide discounted check valves, pressure relief valves, and ball valves for the 5.45 m^3/day experimental prototype that will be presented in the Build & Test report. This prototype will continue to be tested and revised throughout the R&D process, which may require additional purchases from Swagelok. The team will continue fostering this relationship and looks forward to cultivating more partnerships over the years.

B.3 Customer Discovery

In the interest of better understanding the market for wave-powered desalination, Purdue MECC consulted several potential customers within the expansion market, including a coastal landowner and island resort in Greece. Two small-scale seawater desalination companies were interviewed. In doing so, the team was able to clearly identify customer/engineering requirements and their corresponding target values. Chief among them are daily usable water produced and the cost of desalination in Greece and the Caribbean.

B.3.1 Coastal Landowner, Greece

Maher Cherfan is a property owner on the Porto Heli coast of Greece. The water source for his property is a well that collects rainwater and seawater to be desalinated. The initial capital cost of the desalination system was $84,000, in large part due to the drilling needed to find water 65 meters beneath his land. His family only spends around 100 days each year at this estate, during which 24 m^3 of water is consumed each day from the desalination system, for which the total cost is $4,800, amounting to $2.00/$m^3$ of water. Installing the desalination system reduced the cost significantly from the $5.83/$m^3$ previously paid, in which water was delivered by truck from a highly calcified reservoir further inland. Maher's interview provided insight into the customer requirements of Greek coastal landowners: low cost and low maintenance. The government in Porto Heli restricts the intake of water from the sea, hence well drilling is a common method used to access seawater. However, brine waste is currently flushed down another well back to the sea. As desalination's popularity grows among its residents, Porto Heli is increasingly cautious about this practice. It is presumed that Porto Heli and other coastal regions in Greece would be interested in *Osmocean* to reduce cost and electricity consumption.

B.3.2 Small-Scale Seawater Desalination, Greece

Maria Kourempele, a representative of TEMAK Desalination Systems, offered the perspective of a company that specializes in developing desalination systems in Greece. According to Maria, TEMAK's systems have water production capacities ranging from 200 m^3/day to 5,000 m^3/day, with the former being typical of hotels, resorts, and individual residences. In TEMAK's systems, seawater is drawn from beach wells and brine is dissipated into the sea via diffuser pipelines up to 2 km long. This pipe length ensures adequate dilution of brine such that marine environments are left undisturbed. CapEx for the 200 m^3/day plant with energy recovery is $348,000 and OpEx is $1.20/$m^3$. The system lifespan is estimated to be 15 years, typical of most membranes. Finally, Maria highlighted TEMAK's greatest obstacle when installing desalination plants on remote islands: the high cost of importing fossil fuels to run them. From this interview, the team was able to better understand the relevant scale and concluded that the hotel market would be a relevant group of customers.

B.3.3 Island Resort Hotel, Greece

To learn more about the needs of a hotel owner, the team connected with Giorgos Eleftheriadis, manager of the Atlantica Porto Bello Beach Hotel in Kos, Greece. Giorgos provided several technical specifications related to water consumption. Guest and staff rooms, pools, and gardens are supplied by a primary 500 m^3/day RO desalination plant, which operates at an SEC of 3.18 kWh/m^3. A secondary RO unit treats recycled brackish pool water to be reused in the toilets and gardens. For each unit, brine is discharged to the sea after passing through several filters to minimize environmental impact. As sustainability is of concern for the hotel, Giorgos strongly underscored his interest in integrating RO units with wave energy – so long as the large capital investment pays off.

The capital cost for Porto Bello Beach's main RO unit is $600,000. The operational cost is $\$0.80/m^3$. When asked about the most important factors of their desalination system, Giorgos confirmed the expectation that cost is paramount, especially in the wake of COVID-19's damaging impact on the Porto Bello Beach revenue. *Osmocean* effectively couples wave energy with BRO so that all energy required for RO is provided by waves, eliminating the need for expensive grid power.

B.3.4 Small-Scale Seawater Desalination, Caribbean

Dean Bedford is a licensed professional engineer and the president of Gemini Seawater Systems LLC. His company contracts high-efficiency seawater RO projects in the British Virgin Islands, Mexico, and the Bahamas. Gemini systems draw seawater directly from the silty areas of the ocean to prevent disrupting aquatic life, and brine is released at least 1 km from the intake location. One of their plants in Roatán, Honduras is run entirely from solar energy, producing 230 m^3/day while consuming 0.73 kWh/m^3. In addition to deploying small systems in remote communities, Gemini was also contracted to develop a 7500 m^3/day desalination system at the Atlantis resort in the Bahamas. Dean conveyed that this larger system in Atlantis has endured issues with power stability when power outages occur, which is common on the island due to its less-resilient grid. Integrating the desalination plant with inexhaustible wave energy would eliminate this problem.

B.4 Risk Recognition and Management

B.4.1 Associated Risks

There are several risks associated with the development of *Osmocean*. This section delineates these risks as they relate to the environment, human-centered factors, technical implications, and market deployment.

B.4.1.1 Environmental Risks

A major environmental risk associated with desalination systems is the chemical-laden by-product, brine. Brine raises the salinity of ocean water and poses a major risk to ocean life and marine ecosystems. Desalination plants across the world discharge 142 million cubic meters of brine every day, which is a 50% increase from previous estimates [9]. The production and growth of marine organisms is severely affected by the discharge of brine. Since these organisms are interrelated, any distractions in their populations have adverse impacts on all marine life in the area [10]. Brine spills also negatively affect the soil and vegetation, impairing their ability to produce crops and forage [11]. Brine management is hence crucial to mitigate this risk. A future possibility here is to use Pressure Retarded Osmosis (PRO) [22], amongst other brine management techniques.

Another environmental risk associated with *Osmocean*, as any other mechanical system, is the global impact associated with the greenhouse gases released into the atmosphere. Increase in greenhouse gases causes changes in the radiative balance of the Earth that alter climate and weather patterns at global and regional scales [12]. Human health, agriculture, water resources, forests, wildlife, and coastal areas are all in turn vulnerable to climate change [12]. Brine management, PRO, and global impacts such as the Global Warming Potential (GWP) of the system are discussed in further detail in T.10.3: Environmental Impact.

B.4.1.2 Social Risks

Considering the target customer spectrum and primary requirements, balancing stakeholder needs and making considerate trade-offs is the primary social risk associated with *Osmocean*. For instance, economic feasibility is the primary concern for local municipal organizations, one of our three target customers in the expansion market. In contrast, environmental sustainability is the foremost goal for coastal island resorts and non-profit organizations. Local people inhabiting remote island communities require both lower water cost and environmental sustainability.

B.4.1.3 Technical Risks

Osmocean is designed with minimal need for maintenance personnel or oversight. Furthermore, system components were chosen based on long lifespans and ability to operate with seawater. According to the Center for Disease Control and Prevention (CDC), corrosivity can cause damage to system components and lead to contamination of water [13]. As such, stainless steel (SS) 316 was chosen to withstand high desalination pressure and flow rates of salt water.

According to Erik Tynes, an expert in turbochargers design from Energy Recovery™, if run continuously with pretreated water, a turbocharger will have an approximate lifespan of 20 years with minimal large-scale overhaul required. Because of this recommendation, a bag filter was added at the inlet of the system to remove large contaminants that could cause damage to downstream components. Further technical risk mitigation design discussion can be found in T.9.1: System Design for Risk Mitigation.

B.4.1.4 Market Risks

A significant risk of developing a scaled-up wave-powered desalination system is the willingness of customers to invest. For large-scale systems like the Carlsbad Desalination Plant, based on an interview with PhD candidate researcher Quantum Wei, a bank loan is required to finance a significant change in the desalination system. Most capital investors will be wary of sponsoring cutting-edge technology, as empirical data on the performance of the technology is likely to be sparse or non-existent. Banks are thus likely to charge high interest on loans, reducing the margin for error and necessitating a fast return. This leaves the large-scale market nearly impenetrable unless smaller-scale systems are proven feasible.

Even for smaller *Osmocean* deployment, such as in the remote community of Guana Island which requires 75 m^3/day, there are associated market risks. If custom parts like the turbocharger need replacement or maintenance, the remote island may not have sufficient resources, and people will be left without water. For this reason, *Osmocean* was designed to be robust, with a turbocharger lifetime of 20 years and low maintenance required since membrane replacement is only necessary every 5 years.

B.4.2 Social Impact and Opportunities

The *Osmocean* concept is rooted in a motivation to reduce the LCOW, especially in coastal communities with limited access to fresh water. The system has tremendous potential in these areas to create job opportunities which correspond well to the skillsets of the community's members. This job creation includes sectors such as plant operations and transportation.

B.4.3 Failure Maintenance

Twenty-four of the sub-assemblies associated with *Osmocean* use Run-to-Failure (RTF) Maintenance (Figure T.10.0). RTF involves a deliberate plan of remedial actions to be taken post-breakdown [14]. Owing to long product life cycles, most sub-assemblies run to failure and are then replaced with used sub-assemblies following a suitable plan for disposal or reuse. This mode of failure maintenance is especially beneficial since it lowers costs incurred on preventive maintenance, streamlines operations, and eliminates excessive maintenance [14].

B.5 Financial Analysis

B.5.1 Capital Expenditures

The financial analysis is comparable to NREL's paper using the PTO-Sim model [8]. The WEC CapEx was assumed to be the same as NREL's WEC CapEx, $3,880,000 [8], because the WEC used in the Osmo-Sim model (T.4: Overall Modeling Methods) was the same as the 18-meter wide WEC that NREL analyzed.

Total component expenditures for the coupling and BRO components of *Osmocean* were found for a small-scale system of 100 m^3/day from direct product quotes. These include part costs, shipping costs, and a buffer of $3,000 (Table B.5.0).

To find the total BRO CapEx for large scale systems, the budget was assumed to reasonably scale proportionately with the amount of permeate produced. This scaling factor includes construction, deployment labor, and structural materials that are needed to get a total CapEx. For example, for a 100 m^3/day system, the BRO component costs were estimated to be $118,000, but for a 2600 m^3/day system, the CapEx is estimated to be 26 times the price of a 100 m^3/day system, $3,068,000. This number is competitive with the findings of the NREL study, which calculated an RO CapEx of $3,685,000 [8]. For reference, for a 1700 m^3/day RO system in Greece, the estimated CapEx for RO is $3,363,000 according to DesalData, further validating the team's estimate [34].

Table B.5.0: Summary of BRO component costs for *Osmocean* system. Costs are based on quotes from various industry manufacturers and suppliers for a scale of 100 m^3/day of permeate produced.

System Component	Total Cost (USD)
Pumps	$25,000
Turbocharger (Energy Recovery Device)	$20,000
Sensors	$10,000
Valves	$20,000
Pipes and Fittings	$12,000
BRO Membranes (x8)	$6,000
LP Bladder Accumulator	$5,000
BRO Membrane Housing (x2)	$3,000
Bag Filter	$3,000
HP Piston Tank	$2,000
Shipping [25]	$12,000
Total Component Cost	**$118,000**

B.5.2 Operational Expenditures

Operational expenditures for the WEC were also assumed to be the same as NREL assumed, $68,100 [8]. BRO system operational costs are dependent on permeate production capacity (m^3/day). Table B.5.2 lists how the operational costs of BRO are determined, where most factors are like NREL's determination [8], except the membrane costs are multiplied by a factor of 1.2 because BRO systems have increased membrane fouling and require more membrane maintenance. Labor costs are split between direct labor and management labor costs according to equations 7 and 8 in [8], where Cap_{RO} is the capacity of 100 *Osmocean* systems in parallel. Annual water production (AWP) is calculated by multiplying the amount of water produced by 100 systems per day (m^3/day) by the number of days in a year and a capacity factor, which accounts for the fact that the system has a significant amount of downtime.

Table B.5.2: BRO OpEx Costs calculated from NREL's methodology [8] with membrane maintenance costs scaled for BRO. OpEx is calculated for 100 systems in parallel, as is LCOW. This calculation brings the total OpEx RO to $11,150,000.

Direct Labor Costs	$29,700/laborer
Management Labor Costs	$66,000/manager
Spare Parts	$0.04/$m^3$ * AWP * 100
Pretreatment	$0.03/$m^3$ * AWP * 100
Posttreatment	$0.01/$m^3$ * AWP * 100
Membranes	$0.07/$m^3$ * 1.2 * AWP * 100
Insurance	0.5% BRO CapEx * 100
Total	$11,153,000

Plant capacity is assumed to be 49% as found by NREL [8].

B.5.3 Levelized Cost of Water

To determine the economic viability of *Osmocean*, the LCOW was calculated to estimate the overall cost for the system to deliver a cubic meter of water. The LCOW of the *Osmocean* system was determined similarly to NREL's analysis of a WEC-RO system [8]. LCOW is found using equation 1.

$$LCOW = \frac{(FCR * CapEx) + OpEx}{AWP} \quad (1)$$

Here FCR is a fixed charge rate of 10.8% [24], CapEx is the total capital expenditure necessary to deploy the system, OpEx is the operational expenditures of the system per year, and AWP is the annual water production in m^3. The team used a capacity factor for the system's production of 49% to account for changes in sea states, down times, and other losses not accounted for by mathematical modeling.

Table B.5.3: LCOW values for an array of 100 systems in parallel for the *Osmocean* system.

$CapEx_{WEC}$	$387,789,600
$OpEx_{WEC}$	$6,810,700
$CapEx_{BRO}$	$3,068,000
$OpEx_{BRO}$	$11,153,000
AWP	46,198,000
LCOW	**$1.94/ m^3**

The levelized cost of water of the competitive system in NREL's paper was found to be $1.82 [8]. The discrepancy from the paper was discussed with the authors. While the *Osmocean* system LCOW is higher, there are limitations to the mechanical system, given desired simplicity, that are discussed in the technical report in T.9: Optimization Methods and can be improved in future work.

TECHNICAL REPORT

T.1 Introduction

According to the European Union Sustainable Development Goals, 30% of the global population currently lacks reliable access to clean drinking water. Issues such as population growth, climate change, and increased agricultural needs will continue to compound this issue, resulting in the need for novel and more efficient ways to provide cheap and consistent water sources for communities around the world [15]. Currently, reverse osmosis (RO) technologies account for 69% of operational water desalination sites worldwide [16].

Most seawater desalination systems employ continuous RO (CRO), in which seawater traverses multiple RO membrane stages at a constant pressure. The brine is discharged and promptly flushed out of the system. Batch reverse osmosis (BRO) cycles the brine discharge back through the RO system, while varying the pressure and salinity of the feedwater. Figure T.1.0 illustrates the differences in applied pressure for continuous RO and BRO at a feed salinity of 35 g/kg and a permeate flux of 15 L/(m^2-hr) (LMH). As recovery ratio increases, BRO follows the osmotic pressure curve, or minimum instantaneous pressure required to perform RO. This significantly reduces energy expenditures relative to CRO [17,18]. According to Powering the Blue Economy, energy consumption makes up the largest section of operational expenditures for water desalination, at approximately 36% of total operational expenditures [2]. Thus, processes like BRO must be implemented to reduce costs and increase efficiency for desalination sites worldwide.

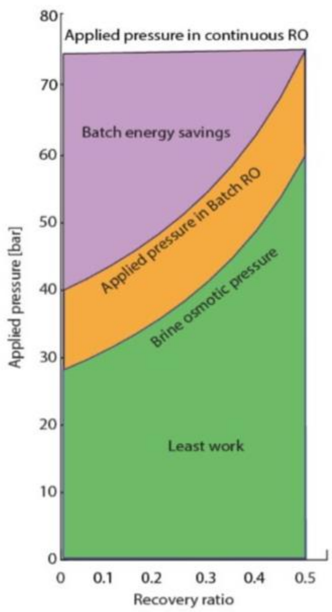

Figure T.1.0: Graphic displaying relevant pressures during the batch process [18]. The area under each curve represents the energy expenditure for each process. The orange section represents the difference between the osmotic pressure curve (green section) and the energy needed for BRO. The purple section is the approximate energy saving BRO produces over CRO [18].

T.2 BRO System Configuration

The Warsinger Water Lab has designed a BRO system (Figure T.2.0) that uses a double acting high pressure piston tank to extract additional energy from recirculated brine. Figure T.1.0 roughly illustrates the change in pressure for one cycle, where a cycle is defined as the transit from a recovery ratio of 0 to the desired final recovery ratio [17]. Recovery ratio is defined as the volume of permeate produced divided by the volume of feedwater added to the BRO system. The high-pressure piston tank operates in 4 stages (Figure T.2.1). During Step A (priming), the piston tank is filled with feed water. The high-pressure pump pumps water at atmospheric pressure and fills the concentrate side of the piston with feed water, and it also fills the pipes and RO module downstream. During Step B (permeate production), the high-pressure pump fills the other side of the tank with new feed water, displacing the piston and forcing fluid through the RO membrane. Within the RO membrane, clean permeate is extracted from the system, while brine is recirculated back through the concentrate side of the piston tank using the circulation pump. At the end of the cycle, the piston reaches the end of the tank, and in Step C (flushing), the system is flushed with feed water, removing the brine from the system. Step D (permeate production) is identical to Step B but opposite in directionality. Feedwater displaces the piston yet again, moving water through the RO module while brine is recirculated.

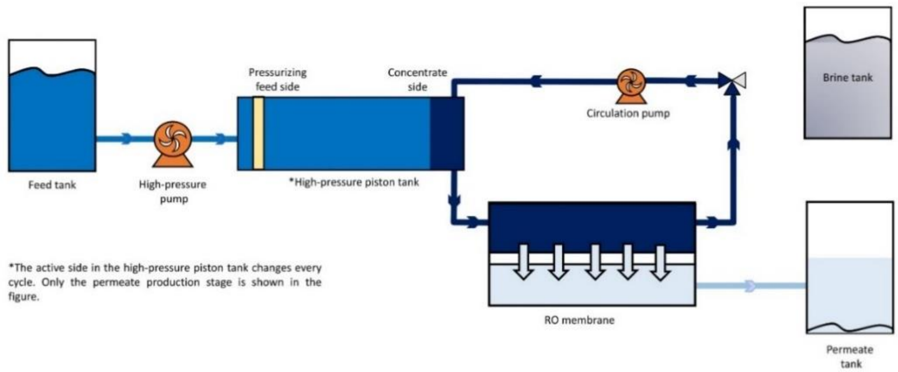

Figure T.2.0: Simplified drawing of the BRO configuration developed by the Warsinger Water Lab. In the permeate production step shown, the piston is forced to the right such that the recently produced brine is further pressurized and recirculated through the membrane [18].

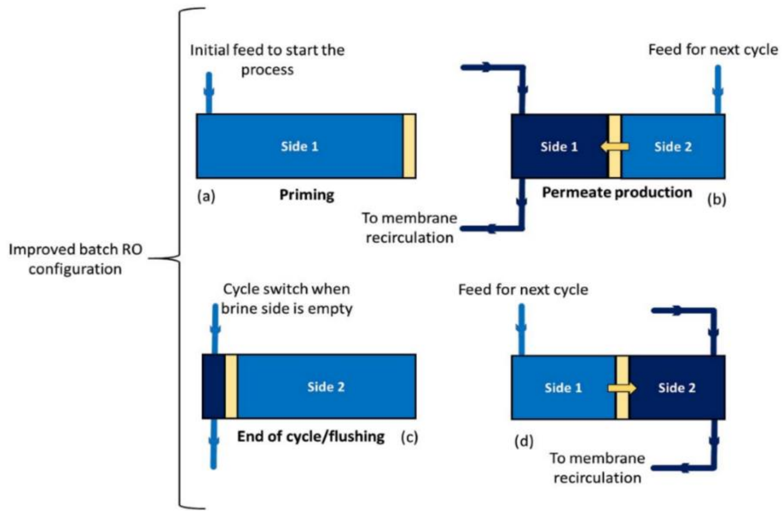

Figure T.2.1: The four-step BRO cycle as experienced in the high-pressure piston tank including (a) Priming, (b) Permeate Production with side 1 active, (c) End of Cycle/Flushing, and (d) Permeate Production with side 2 active [18].

T.3 Proposed Solution

Osmocean is an innovative desalination product combining the efficiencies of BRO with the power potential of wave energy converters (WECs).

At the center of the design is a hydraulic turbocharger. High-pressure flow is passed from the WEC through the hydraulic turbocharger to pressurize pre-filtered seawater for use in a BRO process. Due to the irregular motion of the OSWEC flap, a major design goal was the damping of the energy profile using a kidney loop to both control flowrate and generate electricity. The coupling has an accumulator and optimized controllers, allowing for precise control over the BRO process.

T.4. Overall Modeling Methods

The time-domain simulation model for *Osmocean*, Osmo-Sim, was developed in MATLAB/Simulink and builds upon previous BRO modeling done in the Warsinger Water Lab [18] as well as published wave energy conversion models, WEC-Sim and PTO-Sim [27]. Osmo-Sim (Figure T.4.1) supports the validity of the proposed large-scale physical system (Figure T.4.0), which will be demonstrated at small-scale in the Build & Test Challenge.

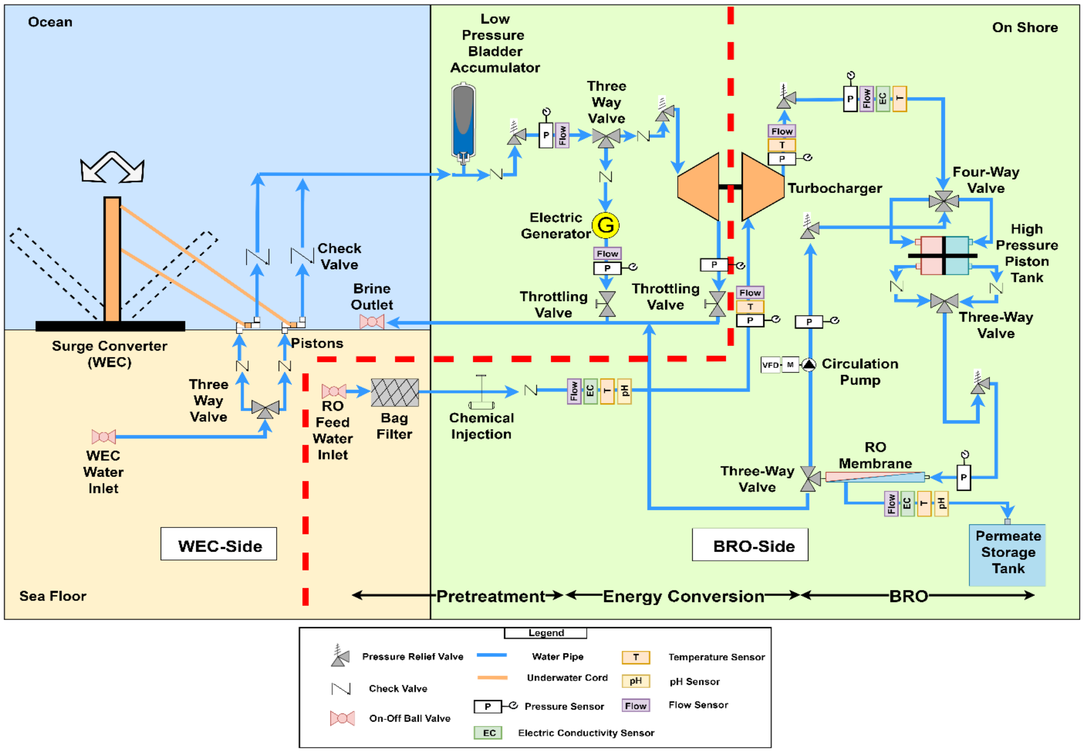

Figure T.4.0: Proposed large-scale physical system P&ID diagram. The system can be divided into two sections: WEC-side and BRO-side. OSWEC motion drives a turbocharger which sends pressurized water to a BRO system for desalination. The turbocharger couples the two sections together.

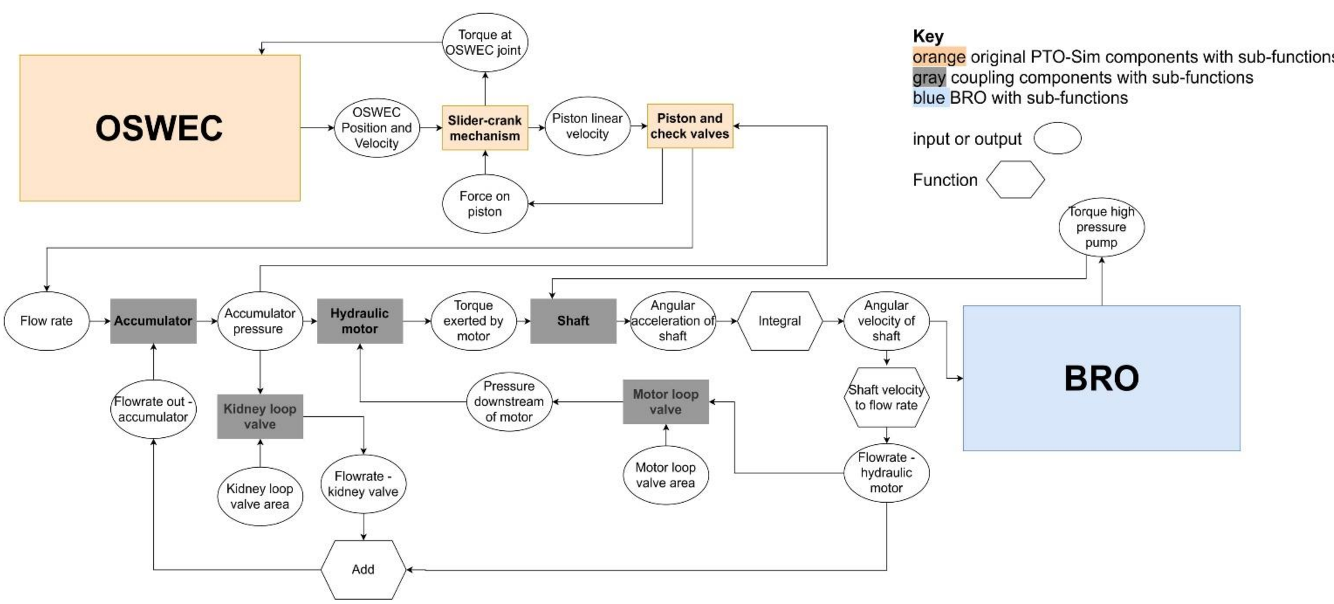

Figure T.4.1: Osmo-Sim model flow chart (excluding controllers). Each component in the system is interdependent with other components via feedback variables. This model was implemented in MATLAB/Simulink.

A flow chart documenting the model is shown in Figure T.4.1. In the model, the turbocharger is represented by a hydraulic motor (Figure T.4.1, gray, center top) coupled to a high-pressure pump (Figure T.4.1, within BRO, blue box) by a shaft connection (Figure T.4.1, gray, top right). There are two controllers in the system. The motor loop valve area (Figure T.4.1, white, bottom right) is controlled to keep the shaft speed of the hydraulic motor constant. The kidney loop valve area (Figure T.4.1, white, bottom left) is controlled to keep the pressure in the accumulator constant.

T.5 Modeling Methods for the WEC and Coupling Systems

T.5.1 Inlet System

The team used the OSWEC example from the WEC-Sim Applications GitHub repository [26], connecting it to the same rotary-to-linear crank mechanism from PTO-Sim [27], in which the slider joint is connected to a piston. The force generated by the motion of the piston sends pressurized seawater through a rectifying check valve, which directs all flow to an accumulator. This accumulator dampens the oscillating flow rate from the WEC, and it is governed by the equation describing a polytropic process of an ideal gas (equation 2), where n can be assumed to equal 1.4 [28]. The output flow from the accumulator is split between the main loop and the kidney loop.

$$V_{\text{accum}} = V_0 * \left(\frac{P_{\text{precharge}}}{P_{\text{accum}}}\right)^{\frac{1}{n}} \tag{2}$$

Here V_{accum} is the instantaneous seawater volume in the accumulator (m^3), V_0 is the initial seawater volume in the accumulator (m^3), $P_{precharge}$ is the precharge pressure of the accumulator (Pa), P_{accum} is the instantaneous gauge pressure of the fluid in the accumulator (Pa), and n is the gas constant.

T.5.2 Kidney Loop

The purpose of the kidney loop valve is to bleed off excess flow from the accumulator outlet, such that the accumulator remains at its rated pressure and volume. Both valves are modeled using the orifice equation (equation 3). A turbulent-characteristic flow coefficient of 0.7 was chosen [29], and the density of seawater was assumed to be 1025 m^3/kg. For this model, orifice size is synonymous with valve area.

$$Q = C_{\text{f}}\Omega\sqrt{\frac{2\Delta P}{\rho}} \tag{3}$$

Here Q is the flow rate through the valve (m^3/sec), C_f is the flow coefficient, Ω is the orifice size (m^2), ΔP is the pressure drop across the valve (Pa), and ρ is fluid density (kg/m^3).

T.5.3 Power Transmission and Control

As water passes through the hydraulic motor in the main loop, hydraulic power is converted to mechanical power. The hydraulic motor is assumed to be a fixed displacement machine (equation 4) and its shaft rotational velocity is governed by a torque balance (equation 5), where back-torque from the high-pressure pump in BRO increases as the membrane pressure increases.

$$nV_{\text{d}} = Q_{\text{main}} \tag{4}$$

Here n is the shaft speed (rev/s), V_d is the volumetric displacement for one rotation of the shaft (m^3/rev), and Q_{main} is the flow rate through the main loop (m^3/sec).

$$\frac{T_{\text{M}} + T_{\text{hpp}}}{2\pi J} = \frac{\Delta P V_{\text{d}}\eta_{\text{m}}/(2\pi) + T_{\text{hpp}}}{2\pi J} = \frac{dn}{dt} \tag{5}$$

Here T_M is the torque acting on the hydraulic motor (N-m), T_{hpp} is the torque acting on the high-pressure pump (N-m), J is the rotational inertia of the shaft (kg-m^2), ΔP is the pressure drop across the hydraulic motor (Pa), η_m is the motor efficiency, and dn/dt is the shaft acceleration (rev/sec^2).

The basis for all valve control is the orifice equation (equation 3). In the case of the main loop throttle valve, the orifice area is modulated to meet a desired hydraulic motor shaft speed by way of PD control. First, the error between the desired and actual shaft speeds is computed (equation 6). Then, the control effort, change in valve area, is found through the definition of PD control (equation 7). The controller gains were chosen experimentally to minimize settling time, overshoot, and chatter.

$$E(s) = R - Y = n_{\text{shaft,ref}} - n_{\text{shaft}} \tag{6}$$

Here $E(s)$ is the error, $n_{\text{shaft,ref}}$ is the desired shaft speed (rev/s) chosen to meet the desired output permeate flux (section T.6), and n_{shaft} is the actual shaft speed (rev/s).

$$\Delta\Omega = E(s)C(s) = E(s)\left(K_p + K_d s\right) \tag{7}$$

Here $\Delta\Omega$ is the necessary change in valve area (m^2) and $C(s)$is the control effort (m^2-sec/rev, for the motor controller).

The kidney loop controller is also a proportional-derivative (PD) controller, wherein the optimal kidney controller gains were obtained experimentally. The error in the kidney loop is described by equation 8, and the change in area is described by equation 7.

$$E(s) = R - Y = p_{\text{h,ref}} - p_{\text{h}} \tag{8}$$

Here $E(s)$ is the error, $p_{\text{h,ref}}$ is the desired accumulator pressure (Pa) which is equal to the rated pressure of the accumulator, and p_{h} is the actual accumulator pressure (Pa).

T.5.4 WEC-Side Assumptions

a. WEC motion is modeled via linear-wave theory, including added mass, radiation damping, and wave excitation components [27].
b. Irregular waves are modeled as a power spectrum of characteristic wave periods [27].
c. Mass of WEC slider-crank links is negligible.
d. Incompressible fluid.
e. One-dimensional, uniform flow.
f. Isothermal system.
g. Minor and major losses in pipes are negligible, and pipe volumes are negligible.
h. Fluid inertia is negligible.
i. Check valves are ideal and do not generate losses.
j. The inputted sea state persists for an entire 24-hour period.
k. Accumulator contains ideal gas.
l. The efficiency of the motor is 0.95 [27].
m. System is initially pre-charged to desired initial conditions: the desired shaft speed, accumulator rated pressure and volume, and both valve areas are initialized at time t = 0 sec.

T.6 Modeling Methods for the BRO System

T.6.1 BRO-Side Overview

As the load on the BRO system increases (i.e. osmotic pressure increases), at constant shaft speed, there is an increasing torque on the shaft connection between the high-pressure pump and the hydraulic motor. The shaft speed from the WEC-side determines the flow rate of the high-pressure pump. From the model's point of view, one cycle is equivalent to one permeate production stage of BRO so flushing is assumed to be instantaneous (Figure T.2.0).

Salinity dynamics calculations occur within an iteration function, which continuously updates the volume and concentration of water in the piston tank over time. The volume and concentrations are re-initialized at the end of each permeate production phase, allowing the simulation of multiple BRO cycles.

T.6.1 Iteration Function: Governing Equations

For the purposes of this BRO model, the flow rate through the high-pressure pump is variable. The high-pressure pump is modeled as a fixed-displacement machine (equation 9) and noting that the high-pressure pump flowrate is equal to the permeate flowrate by conservation of mass, the permeate flux is directly related to the shaft speed (equation 10).

$$Q_{\mathrm{hp}} = nV_{\mathrm{d}} \tag{9}$$

Here Q_{hp} is the flowrate through the high-pressure pump (m^3/sec), n is the shaft angular speed (rev/s), and V_{d} is the volumetric displacement of the high-pressure pump (m^3/rev).

$$J_{\mathrm{w}} = \frac{Q_{\mathrm{p}}}{A_{\mathrm{mem}} n_{\mathrm{ser}} n_{\mathrm{par}}} \tag{10}$$

Here J_{w} is the permeate flux through all membrane modules (m/s), Q_{p} is the total permeate flow rate (m^3/sec), A_{mem} is the membrane area for one module (m^2), n_{ser} is the number of membrane modules in series, and n_{par} is the number of membrane modules in parallel.

The osmotic pressure is the minimum membrane pressure required for reverse osmosis to occur; permeate flux will occur for values of membrane pressure higher than the osmotic pressure (equation 11). Osmotic pressure increases during a BRO cycle as membrane concentration increases. Note that the exponential term accounts for concentration polarization [18]. The mass transfer coefficient was calculated using the Reynolds number – Sherwood number correlation obtained from [33].

$$\pi = iRT * C_{\mathrm{mem}} * e^{\frac{J_{\mathrm{w}}}{k}} \tag{11}$$

Here π is the osmotic pressure (Pa), i is the van't Hoff factor, R is the ideal gas constant (J/mol-K), T is the fluid temperature (K), C_{mem} is the bulk concentration of the fluid (g salt/kg water), and k is the mass transfer coefficient (m^2/s).

The osmotic pressure is related to the feed-side pressure (equal to the high-pressure pump outlet pressure by force balance), the permeate flux, and half of the pressure drop across all membrane modules in series (rightmost term of equation 12).

$$p_{\mathrm{f}} = \frac{J_{\mathrm{w}}}{A_{\mathrm{w}}} + \pi + \frac{f\rho u_{\mathrm{avg}}^2}{4D_{\mathrm{h}}} L_{\mathrm{mem}} n_{\mathrm{ser}} \tag{12}$$

Here p_{f} is the feed-side pressure (i.e. inlet of membrane modules) (Pa), A_{w} is the membrane permeability (m/(s-Pa)), f is the friction factor obtained from [33], ρ is the fluid density (kg/m^3), u_{avg} is the bulk fluid velocity across the membrane (m/s), D_{h} is the hydraulic diameter (m) approximated as twice the spacer thickness [12], and L_{mem} is the length of a single membrane module (m).

Instantaneous torque for a fixed-displacement pump can now be calculated (equation 13), completing the connection between the coupling shaft speed and the torque on the BRO side of the shaft [30]. Here η_{hp} is the high-pressure pump efficiency.

$$T_{\mathrm{hpp}} = \frac{V_{\mathrm{d}} * p_{\mathrm{f}}}{2\pi * \eta_{\mathrm{hp}}} \tag{13}$$

T.6.2 BRO-Side Assumptions

In addition to the assumptions here, the WEC-side assumptions also apply:

a. Calculation is relevant for the permeate production stage of a single cycle of BRO. Energy consumption during flushing step is ignored.
b. The high-pressure tank was sized to provide a final recovery ratio of 0.5, given the total volume of all membrane modules in series and parallel.
c. Mixing in the high-pressure piston tank is instantaneous, such that the bulk concentration in the active side of the tank (C_{f}) is uniform for all time.
d. Acceleration of the high-pressure piston is 0 for all time. In other words, pressure dynamics are negligible relative to salinity dynamics.
e. The high pressure and circulation pumps are fixed-displacement machines with a volumetric efficiency of 1; losses are due to torque inefficiencies.
f. The circulation pump operates at a constant flow rate, fixed to provide the desired instantaneous recovery ratio per pass.
g. When approximating parameters across a branch of modules in series:
    i. Flow parameters are identical for every branch in parallel.
    ii. Bulk concentration in a membrane module increases linearly, from C_{f} to C_{b}, as the flow progresses through a branch.
    iii. Bulk concentration, membrane pressure, flowrate, velocity, and Reynolds numbers are approximated as the average of conditions at the inlet and outlet of the membrane module.

T.7 Results and Validation - WEC-Side

T.7.1 Validation Against Original PTO-Sim

Purdue MECC has validated the WEC-Side of the model in two ways: against published PTO-Sim results [23] and physical intuition. Table T.7.0 provides comparable Osmo-Sim plots to published results [23].

The WEC in Osmo-Sim provides a slightly larger force to the piston (left) than NREL's modeling due to the Osmocean system needing to draw water in from atmospheric pressure. The average absorbed wave power is therefore slightly larger for *Osmocean* (right). The high-pressure pump power (right, BRO Flow Power) increases over each BRO cycle, as expected.

Table T.7.0: Results of Osmo-Sim using the same wave conditions as the plots in [23] – irregular waves with a height of 3 meters and a peak wave period of 11 seconds. The simulation was conducted for a setpoint flux of 30 LMH, 485 membranes in parallel, and 1 in series. Here 10 BRO cycles are plotted.

a. PTO Force (compare to [23] Figure 8)	b. Power (compare to [23] Figure 10, P_{abs} to WEC Input, P_{mech} to Motor Flow, P_{elec} to BRO Flow)
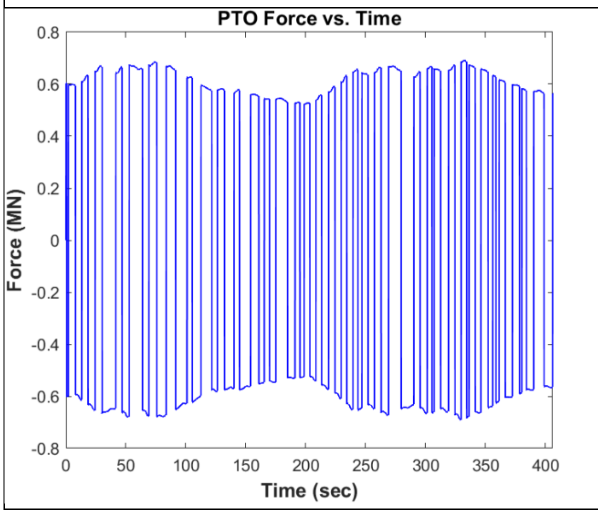	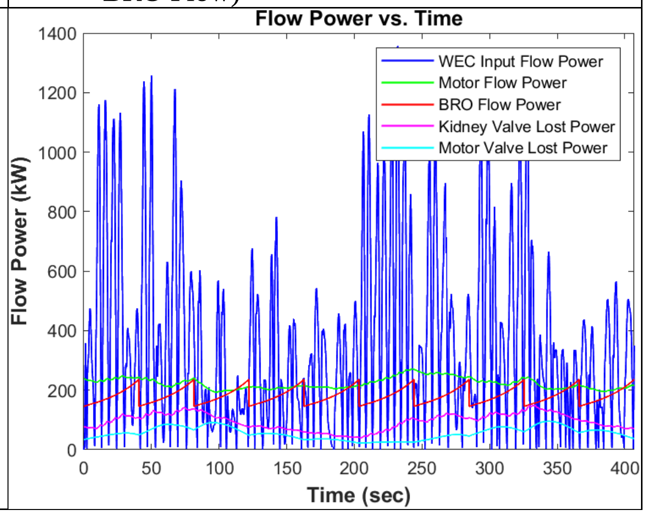

T.7.1 Validation of Control Methods

The accumulator pressure (Table T.7.1, top left) is controlled by the kidney loop throttle valve to match the rated pressure of the accumulator (16 MPa) and to neither exceed its maximum pressure nor drop below its minimum (top left, dashed lines). Comparing to published results, this pressure is on the same order of magnitude as the PTO-Sim accumulator ([23], Figure 9). The kidney valve area (top right, magenta) is changing to control the accumulator pressure: in particular, as the valve's area decreases, the effect based on the orifice equation is to increase the accumulator pressure. Note the dip in accumulator pressure from 100-200 seconds; this coincides with a period of reduced flowrate from the WEC (bottom right, blue) during the same period of 100-200 seconds – here the volume and pressure in the accumulator are decreasing.

The shaft speed (bottom left) is controlled to a constant desired valve by the main loop throttle valve, to achieve a constant desired permeate flux. Despite the rapidly changing inlet flowrate from the WEC, the shaft speed remains within 0.0015% of its desired value, confirming the effectiveness of the motor valve. The corresponding motor valve area (top right, cyan) is changing to control the shaft speed: in particular, when the WEC flowrate is lower than average (from 100-200 seconds), the accumulator pressure is decreasing; thus, for any given pressure drop across the motor, the motor valve has a smaller pressure drop, and must increase its area for a constant flowrate (see the orifice equation).

Consider T.7.1 (bottom right), a plot of the system flowrates. Based on the function of an accumulator, the flow rate out of the accumulator (red) is expected to be a damped version of the flow rate into the accumulator (blue) – which is the case. In addition, the average flow rate out must be equal to the average flow rate in because the accumulator volume must stay roughly constant over time – this is also the case. Note that the flow rate to the main loop is relatively constant (green) and the flow rate out is equal to the sum of the flow rate to the main loop and the flow rate to the kidney loop (pink).

Table T.7.1: Diagnostic plots of Osmo-Sim showing the adequacy of the control method. Identical inputs were used as in Table T.7.0.

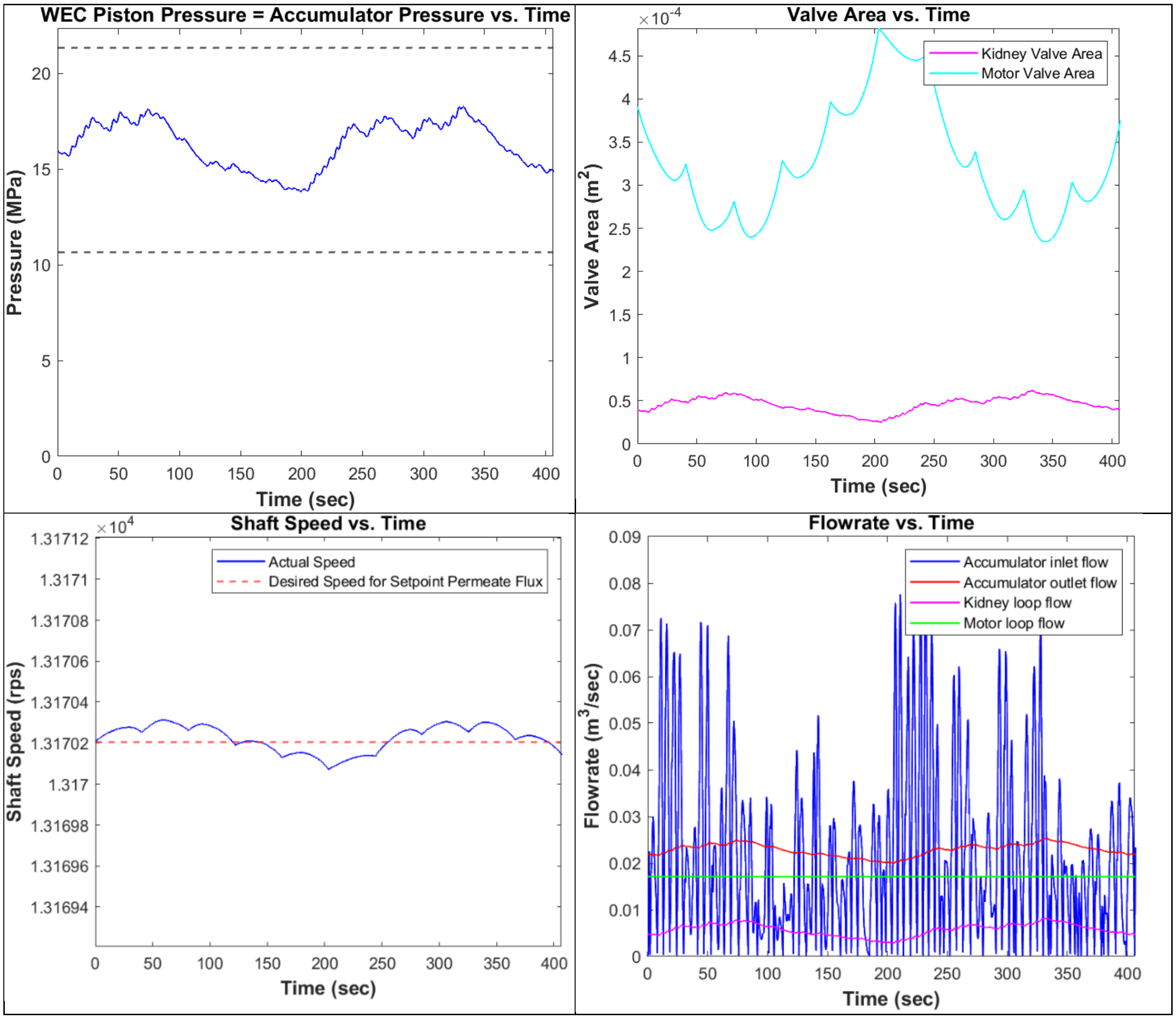

T.8 Results and Validation - BRO-Side

The BRO-side of Osmo-Sim accurately models the BRO process. This is seen in Table T.8.0 (left), which illustrates the feed pressure and osmotic pressure over time. Notably, the feed pressure increases steadily over time while staying a constant amount above the osmotic pressure – this constant pressure difference corresponds to the setpoint permeate flux. Because the recovery ratio increases from 0 to the desired total recovery ratio, this graphic can be thought of as a recreation of Figure T.1.0 above. In this case, the desired flux is set at 30 LMH for a 0.5 total recovery ratio, which corresponds to a maximum high pressure pump pressure of 79 bar. To further confirm the validity of the model, Table T.8.0 (right) shows the piston position over time. The expectation is for piston displacement to reach the stroke length at the end of a cycle. Here, the stroke length is 1 m and the cycle resets when the stroke reaches 95% of its final value - hence, the plot appears as expected. Note that the active side of the tank reverses every BRO cycle.

Table T.8.0: Diagnostic plots of Osmo-Sim showing the adequacy of the BRO-Side. Identical inputs were used as in Table T.7.0.

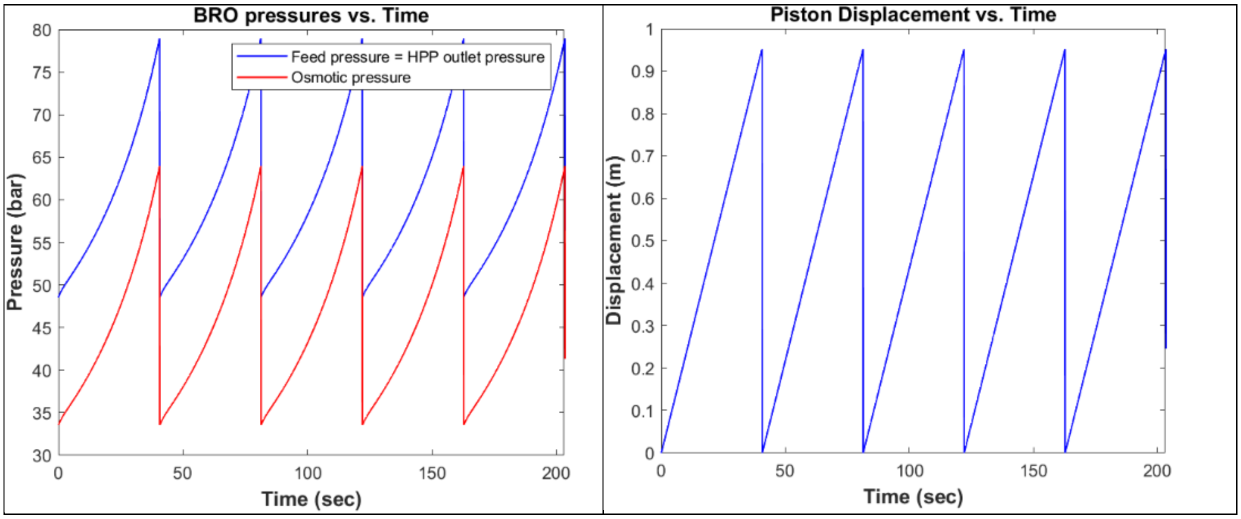

T.9 Optimization Methods

The optimization process of Osmo-Sim involved determining the configuration that would maximize the permeate production of the system. From equation 10, permeate production increases when the any of the following increase: the setpoint permeate flux, the membrane area, and the number of membranes. The setpoint flux is constrained by the maximum allowable feed pressure (equation 12) – corresponding to the burst pressure of the membrane used. For this simulation, the rated working pressure is 80 bar, so the setpoint flux was increased to 30 LMH such that the maximum feed pressure (79 bar) is close to 80 bar. Note that, from equation 12, if modules are added in series, the feed pressure will increase further – hence, all modules were added in parallel.

From simulations, it was noted that increasing membrane area and the number of membranes in parallel has the same effect: the torque on the high-pressure pump increased, hence the pressure drop across the hydraulic motor increased. The *Osmocean* system has two major constraints: the pressure downstream of the motor cannot fall to zero gage (else the motor valve will be unable to exert control effort) and the flowrate through the kidney loop cannot fall to zero (else the kidney valve will be unable to exert control effort). Hence, for a constant rated accumulator pressure, the motor displacement volume was reduced to $1.3*10^{-6}$ m^2 such that the pressure drop across the motor is large, but never enough such that the motor outlet pressure can fall to zero. Thus, there is always a positive pressure difference across the motor valve, but this represents a loss in power (Table T.7.0, right, cyan).

Increasing the number of modules in parallel has the effect of increasing the setpoint shaft speed, hence the equilibrium flow rate through the motor loop. However, the average flowrate provided by the WEC is limited by the sea state: if the flowrate requested by the shaft is higher than the available flowrate, the volume of the accumulator will eventually empty to zero. Hence, the number of membranes in parallel is limited by the sea state, and it must be chosen such that the kidney valve flowrate is positive for all time. Here, the number of membranes in parallel was increased to 485 such that the flowrate through the kidney valve is small, but never zero. Thus, there is always a positive flowrate through the kidney valve, but this represents a loss in power (Table T.7.0, right, magenta).

The model is robust as it can handle different sea states. It was tested for sea states in summer and winter in the Caribbean and in Greece for irregular waves and sea states varying from wave heights of 1-1.75 m and peak periods of 5.5-9.25 seconds [36]. It was found that a larger amount of permeate could be produced in sea states for which the wave height is larger, corresponding to the results in [8].

The specific energy consumption of the *Osmocean* system was calculated by dividing the average absorbed power of the WEC, 366 kW, by the permeate production flow rate, 0.03 m^3/sec, and converting to kWh to get a total system SEC of 3.43 kWh/m^3. This high SEC is due to a mechanical simplification of the wave energy conversion system, which assumes the input accumulator is connected to the ambient pressure and results in a WEC efficiency of 60%. However, previous work has shown how implementing BRO can have up to 60% energy savings when compared to a continuous RO system [18].

While this SEC is higher than published SECs of wave-to-RO systems, 2.0 kWh/m^3 [35] and NREL's 2.8 kWh/m^3 [2], future work could focus on lowering the SEC of the system by investigating closing the working fluid system of the WEC, similar to the Resolute Marine solution [31] to improve the overall efficiency, although the mechanical simplicity and environmental benefits of the *Osmocean* system would be compromised. Closing the loop, by adding a second accumulator in place of the kidney loop and adding a generator in place of the main loop throttle valve, would provide a possible avenue of improvement as it would allow the WEC to build a higher working pressure for the hydraulic motor. This replacement for the throttle valve will control the work generated by modifying the back emf of the generator, allowing for full system control while maximizing energy utilization.

There is a design tradeoff in *Osmocean* between the flux and SEC required, which is likely the second reason SEC is high for the *Osmocean* system. In Table T.9.0, it can be seen how a flux of 30 LMH results in a greater SEC, especially at lower PTO efficiencies.

Table T.9.0: According to BRO models from the Warsinger Water Lab [17,18,38], the SEC of *Osmocean* decreases with increasing wave energy conversion efficiency and decreasing flux (Left: 15 LMH, Right: 30 LMH). In Osmo-Sim, the total recovery ratio is 0.5, and the recovery ratio per pass is 0.1. In these plots, seawater salinity is assumed to be 35 g/kg. WEC inefficiencies are applied to both pumps. WEC efficiency is defined as the high-pressure pump shaft power divided by the WEC absorbed power.

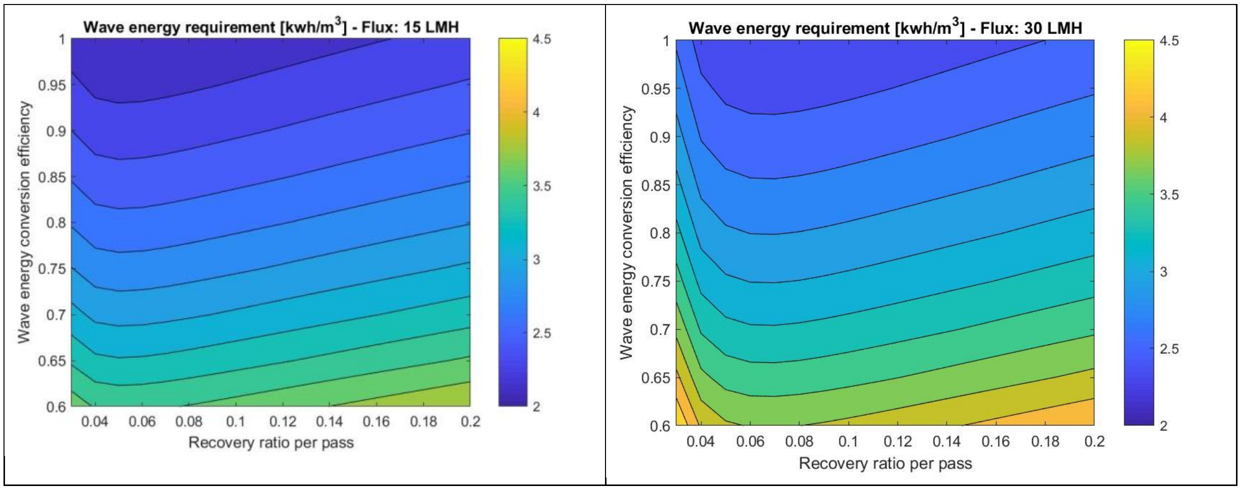

T.9.1 System Design for Risk Mitigation

Osmocean has several components that operate at high pressures, necessitating a thorough risk mitigation analysis. The WEC system operates at a nominal 150 psi which requires piping that can provide an adequate factor of safety while balancing system cost. The team determined that the minimum factor of safety (FOS) that the system must meet is 2.0. The team initially chose 316 stainless steel for the 3-inch pipes for its long lifetime and maximum rated pressure, providing a FOS of 8.67. This is significantly higher than design requirements. However, the high cost of about $44 per ft encouraged the team to choose an alternative material: Schedule 40 PVC. This type of piping has a pressure rating of 260 psi, producing a FOS of 1.73. PVC also has the advantage of significantly lower cost per foot of about $2. The team produced one final iteration, sizing the pipe down from 3 inches to 2 ½ inches, providing a pressure rating of 300 psi and a FOS of 2.0, meeting design criterion.

T.9.2 Pipe Loss Calculations

Both the major and minor losses in the pipes of the system were accounted for using Osmo-Sim data to give an accurate pressure drop at each critical location, specifically at the hydraulic motor and at the kidney loop throttling valve. To find these pipe losses, the system was divided into three sections, the inlet, the kidney loop, and the hydraulic generator loop, with pipe lengths and tabulated losses calculated for each section. The flow rate and pressure out from the accumulator were used to find a mass flow rate and a bulk fluid velocity for each section using the design goal of prototype is to have roughly 90% of the WEC flow going through the hydraulic motor. The remaining 10% passes through the kidney loop, providing the system with energy to run both control systems. This bulk velocity was used to find the Reynolds number using seawater properties, allowing the Darcy Friction Factor to be found for the section using a Moody diagram and the surface roughness to be found from a lookup table for turned stainless steel pipe [32]. The range of friction factors was sufficiently small to use a single friction factor to characterize the system using a weighted average of the Reynolds numbers. This friction factor was used in the Darcy-Weisbach Equation to determine the major pressure losses.

The minor pressure losses were determined using loss coefficients [32] and combined using to calculate a pressure loss for the components. The major and minor pressure losses were then combined and subtracted from the inlet pressure to determine the per component pressures. The pressure drops across the inlet and hydraulic motor are 10 kPa. The pressure drop across the kidney loop is 0.13 kPa for an average run, which is very small compared to other losses. Therefore, the pressure drops are negligible.

T.10 Environmental Methods and Results

T.10.1 Methods

A life cycle assessment (LCA) was performed to assess the environmental impacts associated with various stages of *Osmocean*'s life using SimaPro. The LCA flowchart (Figure T.10.0) outlines each sub-assembly analyzed for the product life cycle. Considering the project constraints, the scope of the LCA was limited to manufacturing materials, transportation, and waste disposal. Manufacturing processes, while crucial to a life cycle assessment, were excluded from the scope due to the complexity involved with the many sub-assemblies. Environmental inputs for the life cycle inventory (LCI) were obtained from companies manufacturing and supplying each part for the small-scale design which corresponds to a maximum flow rate of 100 m^3/day. The procurement and transport map (Figure T.10.1) highlights the path of each part from its parent location to West Lafayette, Indiana and ultimately to its destination in Guana Island, BVI, part of the expansion market.

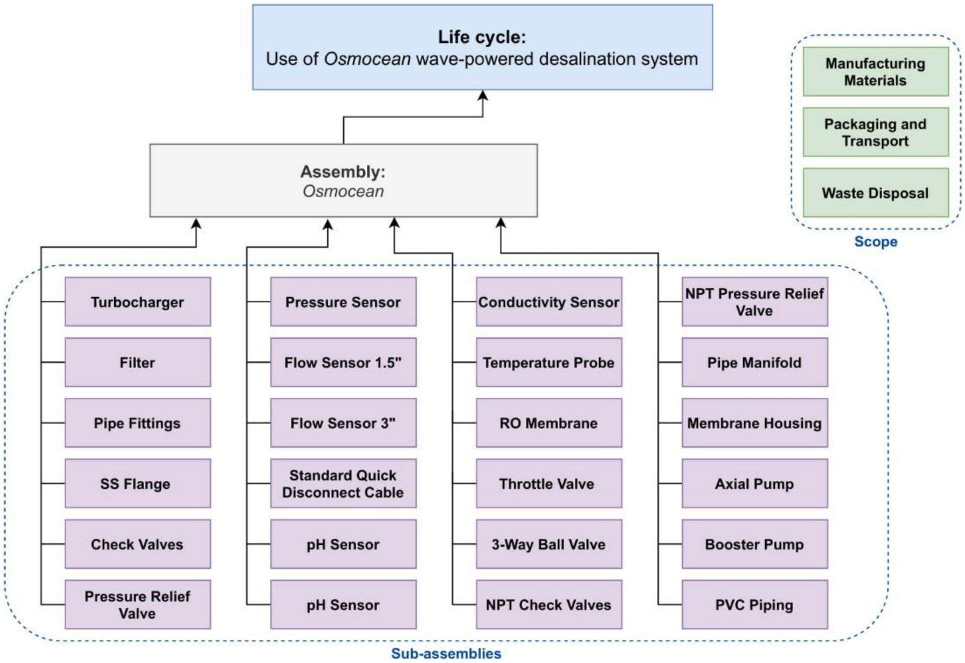

Figure T.10.0: Life cycle analysis flow chart for the *Osmocean* assembly. Outlined here are the twenty-four sub-assemblies and the scope of the assessment.

T.10.2 Assumptions

Based on the environmental inputs received from manufacturers and suppliers, several significant assumptions were made for the system's LCA. For the scope of transport, it was assumed that all parts were to be transported to Guana Island, British Virgin Islands (BVI). This choice of community correlated most closely to *Osmocean*'s target market and required an average flow rate of 75 m^3/day, which can be provided by the small-scale design. For each part, the environmental impact of transportation was determined for travel to West Lafayette, Indiana from the location where parts were manufactured or supplied. Once in West Lafayette, the transportation was assumed to be via truck to Chicago O'Hare, then transported to West Palm Beach, Florida by air freight. From West Palm Beach, the parts are assumed to be transported to Tortola by cargo ship, then sent to Guana Island, BVI by barge.

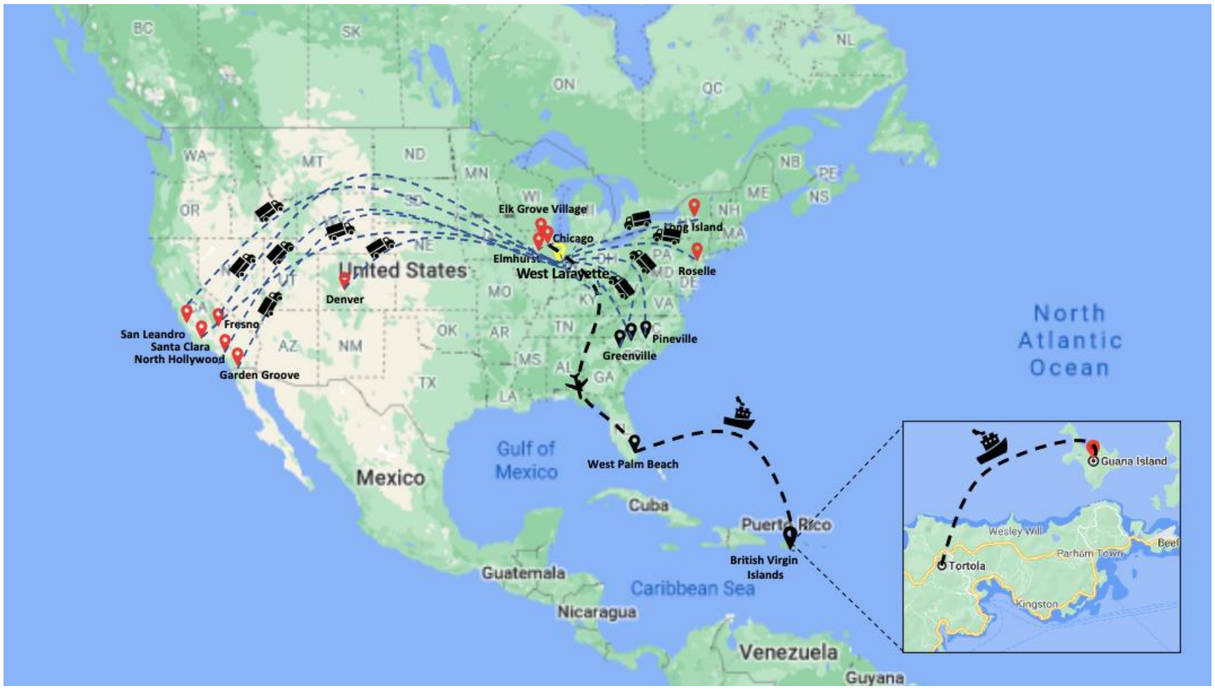

Figure T.10.1: Procurement and transport map showing the route of each sub-assembly from the manufacturing location to West Lafayette, Indiana and ultimately to Guana Island, BVI. Excluded here but included in the LCA are two sub-assemblies procured from Fujian Province, China and East Yorkshire, England.

T.10.3 Environmental impact of *Osmocean*

Stainless Steel (SS) 316 is a primary component of most sub-assemblies in the system. This grade of austenitic stainless steel is particularly effective in thermal desalination applications due to its resistance to high temperatures and corrosive environments [19]. It also has a high recyclability potential owing to its high intrinsic value. Furthermore, stainless steel is a very long-lasting material. This substantially reduces the energy demands during the production of new material, making it a very sustainable material [20].

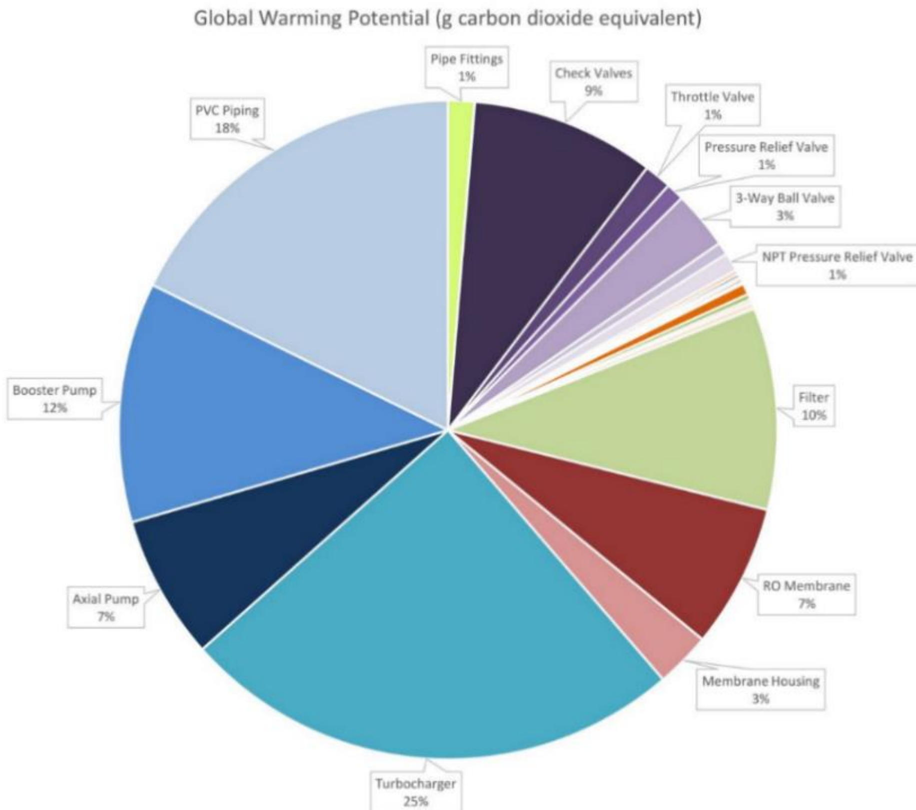

Figure T.10.2: Global Warming Potential contributions of each *Osmocean* sub-assembly. The total GWP for the large-scale assembly is 3630 kg equivalent of CO_2. Only sub-assemblies with a non-zero GWP contribution are shown here (sensors have a near zero percent contribution to the total GWP).

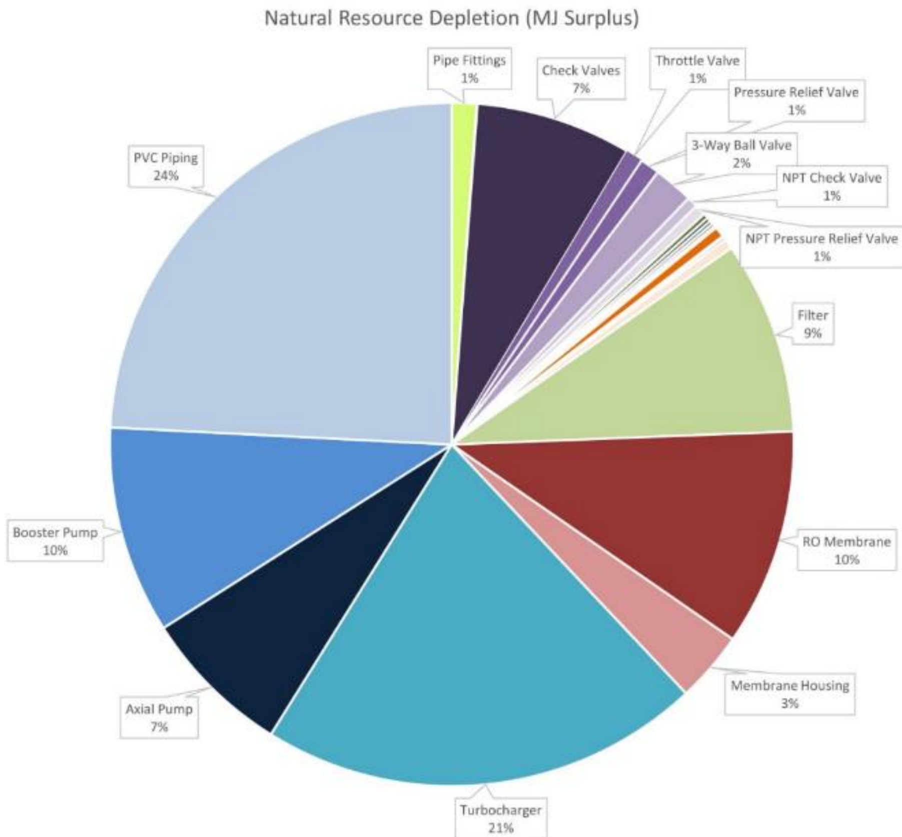

Figure T.10.3: Natural Resource Depletion contributions of each *Osmocean* sub-assembly. The total NRD for the large-scale assembly is 6061 MJ Surplus. Only sub-assemblies with a non-zero NRD contribution are shown here (sensors have a near zero percent contribution to the total NRD).

The Global Warming Potential (GWP) was assessed for the *Osmocean* assembly (Figure T.10.2). The system has a total 3630 kg CO_2 equivalent of GWP with the turbocharger (21%), PVC piping (18%), and booster pump (12%) making the highest contributions. The LCA was also used to assess the exhaustion of natural resources or the Natural Resource Depletion (NRD) for the system (Figure T.10.3). A total of 6061 MJ Surplus of NRD was found to be associated with the assembly. The PVC piping (24%), turbocharger (21%), booster pump (10%) and RO membranes (10%) made the more significant contributions here. Considering the product lifespan of 20 years, these are considered by the Environmental Protection Agency to be sufficiently low values of GWP and NRD [37].

A major waste associated with desalination technologies is brine. Due to its high concentration of salt and contaminants, proper brine management is crucial to environmental sustainability. The main options for managing brine fall under two categories: brine treatment for reuse and brine disposal [21]. A future outlook for *Osmocean* is to further sustainability by incorporating Pressure Retarded Osmosis (PRO) for energy recovery using brine. PRO involves pumping of low salinity feed and high salinity brine across opposite sides of the membrane. This creates an osmotic pressure gradient which draws feed through to collect permeate. Finally, a hydro turbine depressurizes the draw stream to recover energy [22].

T.11 Customer Discussion

The remote resorts and small island communities which make up *Osmocean*'s expansion market have expressed interest in making their water source less impactful on the environment. This concept draws from tourism's growing concern for sustainability as well as environmental regulations by governing states. However, unless the cost is significantly reduced, the prospect of integrating more sustainable solutions is unlikely. Quantum Wei, a researcher of batch reverse osmosis techno-economics at MIT, recounted that a 10% reduction in LCOW would influence the customer to invest in a new system. The techno-economic analysis of *Osmocean* determined an LCOW of $1.94/m^3. This LCOW is not smaller than published values, but this is due to a mechanical limitation which will be investigated in future work.

Conclusions

Purdue MECC concluded, through business analysis and the Osmo-Sim model, that a wave-powered BRO desalination system with the *Osmocean* coupling is an exciting new alternative to wave-powered RO systems currently using electricity generation. The model has been validated against published papers, and has led to three primary conclusions:

1. Wave-powered BRO is competitive, feasible, and practical, though it needs further optimization. Currently, the model produces the lowest LCOW, $1.94 dollars/m^3, at 2600 m^3/day [40].
2. The initial target market for *Osmocean* is existing WEC and WEC-RO developers, as the system is most financially viable when reducing energy consumption of existing RO or adding the *Osmocean* coupling to existing WEC systems.
3. There is significant expansion potential to market to remote island communities and local municipalities due to their need for sustainable systems and more efficient RO.

Future work for the development of *Osmocean* will include the following:

1. Improving system performance by closing the loop, in place of the current solution where water is drawn from atmospheric pressure into the system by the WEC.
2. Validating different membrane configurations for BRO to better optimize energy consumption, and LCOW.
3. Integrating Pressure Retarded Osmosis (PRO) [22] into the *Osmocean* system to optimize brine management while also recovering energy.

Osmocean is the most innovative wave-desalination system on the market, and future work will ensure that it is the most efficient and cost-effective option for coastal communities.

References

1. Fact Sheet: People and Oceans. (2017). *The Ocean Conference, United Nations*. Retrieved from https://www.un.org/sustainabledevelopment/wp-content/uploads/2017/05/Ocean-fact-sheet-package.pdf
2. LiVecchi, A., A. Copping, D. Jenne, A. Gorton, R. Preus, G. Gill, R. Robichaud, R. Green, S. Geerlofs, S. Gore, D. Hume, W. McShane, C. Schmaus, H. Spence. 2019. *Powering the Blue Economy; Exploring Opportunities for Marine Renewable Energy in Maritime Markets*. U.S. Department of Energy, Office of Energy Efficiency and Renewable Energy. Washington, D.C.
3. Resolute Marine Limited Clean Water From Ocean Waves. (2015). *MRIA Ocean Energy Industry Forum*. Retrieved from http://mria.ie/documents/503badd7d6904035e510fed4a.pdf
4. Why wavepiston will make wave power competitive. (n.d.). Retrieved from https://wavepiston.dk/download/why.pdf.
5. Ahmadi, E., McLellan, B., Ogata, S., Mohammadi-Ivatloo, B., & Tezuka, T. (2020). An integrated planning framework for sustainable water and energy supply. *Sustainability (Switzerland)*, *12*(10). https://doi.org/10.3390/su12104295
6. Tzen, E. (2018). Wind-Powered Desalination-Principles, Configurations, Design, and Implementation. In *Renewable Energy Powered Desalination Handbook: Application and*

Thermodynamics (pp. 91–139). Elsevier Inc. https://doi.org/10.1016/B978-0-12-815244-7.00003-9

7. Kaya, A., Evren Tok, M., & Koc, M. (2019). A levelized cost analysis for solar-energy-powered sea water desalination in the Emirate of Abu Dhabi. *Sustainability (Switzerland)*, *11*(6). https://doi.org/10.3390/su11061691
8. Yu, Y. H., & Jenne, D. (2017). Analysis of a wave-powered, reverse-osmosis system and its economic availability in the United States. In *Proceedings of the International Conference on Offshore Mechanics and Arctic Engineering - OMAE* (Vol. 10). American Society of Mechanical Engineers (ASME). https://doi.org/10.1115/OMAE2017-62136
9. McGrath, M. (2019). Concerns over increase in toxic brine from desalination plants. Retrieved from https://www.bbc.com/news/science-environment-46863146.
10. Ahmed, Musfique & Anwar, Rifat. (2012). An Assessment of the Environmental Impact of Brine Disposal in Marine Environment. International Journal of Modern Engineering Research. 24. 2756-2761.
11. Meehan, M., Sedivec, K., Desutter, T., Augustin, C., Daigh, A., Livestock, E., … Daigh, A. (2017). Environmental Impacts of Brine (Produced Water). *North Dakota State University*, (June), 1–4. Retrieved from https://www.ag.ndsu.edu/publications/environment-natural-resources/environmental-impacts-of-brine-produced-water/r1850.pdf
12. What are the trends in greenhouse gas emissions and concentrations and their impacts on human health and the environment? (n.d.). Retrieved from https://www.epa.gov/report-environment/greenhouse-gases.
13. Drinking water Pipe Systems. (2013, July 10). Retrieved from https://www.cdc.gov/fluoridation/engineering/corrosion.html
14. Run-to-Failure vs. Breakdown Maintenance. (2020). Retrieved from https://www.getmaintainx.com/learning-center/run-to-failure-vs-breakdown-maintenance/.
15. Clean Water and Sanitation. (n.d.). *European Commission, International Partnerships*. Retrieved from https://ec.europa.eu/international-partnerships/sdg/clean-water-and-sanitation_en.
16. Jones, E., Qadir, M., Vliet, M., Smakhtin, V., MuKang, S. The state of desalination and brine production: A global outlook. Science of the Total Environment 657 (2019), 1343-1356.
17. Cordoba, Sandra P., Das, Abhimanyu, and Warsinger, David M., "Improved Batch Reverse Osmosis Configuration for Better Energy Efficiency" (2019). *IDA World Congress, Abu Dhabi, UAE, October 20-24, 2019*.
18. Cordoba, S., Das, A., Leon, J., Garcia, J. M., & Warsinger, D. M. (2021). Double-acting batch reverse osmosis configuration for best-in-class efficiency and low downtime. *Desalination*, *506*. https://doi.org/10.1016/j.desal.2021.114959
19. Panagopoulos, A., Loizidou, M., & Haralambous, K. J. (2020, October 1). Stainless Steel in Thermal Desalination and Brine Treatment: Current Status and Prospects. *Metals and Materials International*. Korean Institute of Metals and Materials. https://doi.org/10.1007/s12540-019-00398-w
20. Is Stainless Steel Sustainable or Bad for the Environment? (n.d.). *Tiny Eco Home Life*. Retrieved from https://www.tinyecohomelife.com/is-stainless-steel-sustainable-environment.
21. How to Treat Brine Disposal and Management. (2017). *Saltworks*. Retrieved from https://www.saltworkstech.com/articles/how-to-manage-brine-disposal-and-treatment/.
22. Rao, A. K., Li, O. R., Wrede, L., Coan, S., Elias, G., Cordoba, S., Roggenberg, M., Castillo, L. Warsinger, D. M., PhD.(n.d.). A Framework for Producing Blue Energy from Reverse Osmosis Desalination. *Desalination,* vol 511, pp 115088, https://doi.org/10.1016/j.desal.2021.115088
23. So, R., Casey, S., Kanner, S., Simmons, A., & Brekken, T. K. A. (2015). PTO-Sim: Development of a power take off modeling tool for ocean wave energy conversion. In *IEEE Power and Energy Society General Meeting* (Vol. 2015-September). IEEE Computer Society. https://doi.org/10.1109/PESGM.2015.7285735

24. Yu, Y. H., Jenne, D. S., Thresher, R., Copping, A., Geerlofs, S., & Hanna, L. A. *Reference Model 5 (RM5): Oscillating Surge Wave Energy Converter*. United States. https://doi.org/10.2172/1169778
25. AMID Logistics, LLC. U.S. Sea Freight Price Calculator. https://internationalshippingusa.com/home.aspx?cnts=260&refcntr=1&ref=p181207_013E1cwqfAZ#.YHd5mxRKjCU
26. WEC-Sim Applications Repository. (n.d.). Retrieved from https://github.com/WEC-Sim/WEC-Sim_Applications
27. WEC-Sim. (2020). *National Renewable Energy Laboratory and National Technology & Engineering Solutions of Sandia*. Retrieved from http://wec-sim.github.io/WEC-Sim
28. Vacca, A., PhD. (spring 2019). *ME 597/ ABE 491 Design and Modeling of Fluid Power Systems, Lecture 9 - Accumulators* [PDF].
29. Vacca, A., PhD. (spring 2019). *ME 597/ ABE 491 Design and Modeling of Fluid Power Systems, Lecture 2 - Equations and Orifice* [PDF].
30. Vacca, A., PhD. (spring 2019). *ME 597/ ABE 491 Design and Modeling of Fluid Power Systems, Lecture 6 - Pumps and Motors for Fluid Power Applications* [PDF].
31. Reavis, C., & Zuckerman, E. (2014). Resolute Marine Energy: Power in Waves. *MIT Management Sloan School*. Retrieved from https://mitsloan.mit.edu/sites/default/files/2020-03/RME Power in Waves.IC_.pdf.
32. Pritchard, P. J., & Mitchell, J. W. (n.d.). *Fox and McDonald's Introduction to Fluid Mechanics, 9th Edition*.
33. Park, K., Burlace, L., Dhakal, N., Mudgal, A., Stewart, N. A., & Davies, P. A. (2020). Design, modelling and optimisation of a batch reverse osmosis (RO) desalination system using a free piston for brackish water treatment. *Desalination*, *494*. https://doi.org/10.1016/j.desal.2020.114625
34. Cost Estimator: DesalData. (n.d.). Retrieved from https://desaldata.com/cost_estimator.
35. Folley, M., & Whittaker, T. (2009). The cost of water from an autonomous wave-powered desalination plant. Renewable Energy, 34(1), 75–81. https://doi.org/10.1016/j.renene.2008.03.009
36. Ribal, A. & Young, I. R. (2019). 33 years of globally calibrated wave height and wind speed data based on altimeter observations. *Nature*. https://www.nature.com/articles/s41597-019-0083-9.pdf
37. Greenhouse Gas Emissions. (n.d.). *Unite States Environmental Protection Agency*. Retrieved from https://www.epa.gov/ghgemissions/understanding-global-warming-potentials.
38. Das, A. and Warsinger, D.M., 2021. Batch counterflow reverse osmosis. *Desalination*, 507, p.115008. https://doi.org/10.1016/j.desal.2021.115008
39. E. W Tow, A. L. Hartman, A. Jaworowski, I. Zucker, S. Kum, M. AzadiAghdam, E. R Blatchley III, A. Achilli, H. Gu, G. M. Urper, David M Warsinger, Modeling the energy consumption of potable water reuse schemes, Water Research X, vol. 13, pp. 100126, 2021 (doi link) https://doi.org/10.1016/j.wroa.2021.100126
40. K. M. Brodersen, E. A. Bywater, A. M. Lanter, H. H. Schennum, K. N. Furia, M. K. Sheth, N. S. Kiefer, B. K. Cafferty, A. K. Rao, J. M. Garcia., D. M. Warsinger, Direct-drive ocean wave-powered batch reverse osmosis, *Desalination*, vol. 23, 15393, 2022 https://doi.org/10.1016/j.desal.2021.115393

Acknowledgements

The Purdue MECC 2021 team would like to thank Dr. José Garcia, Dr. Luciano Castillo, and Helber Antonio Esquivel Puentes for providing valuable inputs on design and modeling, Dr. Fu Zhao for his advice on the life cycle assessment, and all manufacturers and suppliers for providing environmental inputs for all sub-assemblies.